IL-25 and type 2 innate lymphoid cells induce pulmonary fibrosis

Emily Hams[a,b], Michelle E. Armstrong[a,b], Jillian L. Barlow[c], Sean P. Saunders[a,b], Christian Schwartz[d], Gordon Cooke[e], Ruairi J. Fahy[f], Thomas B. Crotty[g], Nikhil Hirani[h], Robin J. Flynn[c], David Voehringer[d], Andrew N. J. McKenzie[c], Seamas C. Donnelly[e,i], and Padraic G. Fallon[a,b,j,1]

[a]Trinity Biomedical Sciences Institute, School of Medicine, Trinity College Dublin, Dublin 2, Ireland; [b]National Children's Research Centre, Our Lady's Children's Hospital, Dublin 8, Ireland; [c]Medical Research Council Laboratory of Molecular Biology, Cambridge CB2 0QH, United Kingdom; [d]Department of Infection Biology, Universitätsklinikum Erlangen, 91054 Erlangen, Germany; [e]School of Medicine and Medical Science, University College Dublin, Dublin 4, Ireland; [f]St. James's Hospital, Dublin 8, Ireland; [g]Department of Pathology, St. Vincent's University Hospital, Dublin 4, Ireland; [h]Medical Research Council Centre for Inflammation Research, University of Edinburgh, Edinburgh EH16 4SB, United Kingdom; [i]National Pulmonary Fibrosis Referral Centre, St. Vincent's University Hospital, Dublin 4, Ireland; and [j]Institute of Molecular Medicine, School of Medicine, Trinity College Dublin, St. James's Hospital, Dublin 8, Ireland

Edited by Shigeo Koyasu, RIKEN Center for Integrative Medical Sciences, Yokohama, Japan, and accepted by the Editorial Board November 15, 2013 (received for review August 26, 2013)

Disease conditions associated with pulmonary fibrosis are progressive and have a poor long-term prognosis with irreversible changes in airway architecture leading to marked morbidity and mortalities. Using murine models we demonstrate a role for interleukin (IL)-25 in the generation of pulmonary fibrosis. Mechanistically, we identify IL-13 release from type 2 innate lymphoid cells (ILC2) as sufficient to drive collagen deposition in the lungs of challenged mice and suggest this as a potential mechanism through which IL-25 is acting. Additionally, we demonstrate that in human idiopathic pulmonary fibrosis there is increased pulmonary expression of IL-25 and also observe a population ILC2 in the lungs of idiopathic pulmonary fibrosis patients. Collectively, we present an innate mechanism for the generation of pulmonary fibrosis, via IL-25 and ILC2, that occurs independently of T-cell–mediated antigen-specific immune responses. These results suggest the potential of therapeutically targeting IL-25 and ILC2 for the treatment of human fibrotic diseases.

innate response | cytokine | therapy | inflammation

Disease conditions associated with pulmonary fibrosis are often progressive and have a poor long-term prognosis (1). In the context of developing new treatments for pulmonary fibrosis, the cytokines associated with the pathogenic milieu that can lead to aberrant extracellular matrix deposition are key targets, in particular interleukin (IL)-13, TGF-β, and, more recently, IL-17A (2). However, to develop more effective therapeutics for fibrotic lung diseases a greater understanding of the pathogenesis and the underlying mechanisms that lead to pulmonary fibrosis is needed (3, 4).

The cytokine IL-13 was first implicated in fibrosis using profibrotic eggs from the type 2 cytokine-inducing pathogen *Schistosoma mansoni*, in the presence of a soluble IL-13Rα2-Fc fusion protein (5) and in *Il13*$^{-/-}$ mice (6). IL-13 is now widely linked to a range of fibrotic conditions (7) including asthma, where IL-13 is being targeted as a therapy (8). In the context of the cellular source of IL-13 in the generation of fibrosis, CD4^{+} T helper (h) 2 cells are implicated (9). However, more recently innate lymphoid cells (ILC) are emerging as an important source of IL-13 (10, 11). In this context, the type 2 cytokine IL-25 is implicated in the generation of the recently identified IL-13–expressing ILC, termed ILC2 (11–14).

Recent studies have implicated IL-25 and ILC2 in the pathogenesis of pulmonary conditions in both murine models and human conditions such as allergic asthma (12, 13, 15, 16). In murine studies intranasal administration of IL-25 results in evidence of pulmonary tissue remodeling including development of perivascular fibrosis, and intratracheal administration results in increased pulmonary Th2 cytokines and airways hyper-reactivity (AHR) (17, 18), whereas blocking IL-25 reduces AHR severity (19). Herein we describe a potential role for IL-25 in the generation of pulmonary fibrosis in experimental mouse models, via the activation of IL-13–producing ILC2. We also observe increases in both IL-25 and ILC2 in the lung of patients with idiopathic pulmonary fibrosis (IPF). These data suggest unique mechanisms for the generation of pulmonary fibrosis and identify an interesting area for further research on the role of IL-25 and ILC2 in the treatment of pulmonary fibrosis.

Results

Mice Unable to Signal via IL-25 Show Decreased *S. mansoni* Egg-Associated Pulmonary Fibrosis. To address the mechanistic role of IL-25 in pulmonary fibrosis we used the *S. mansoni* egg-induced pulmonary granuloma model. In mice deficient in IL-25 (*Il25*$^{-/-}$) and its receptor IL-17BR (*Il17br*$^{-/-}$) there was smaller egg granuloma formation relative to WT mice (Fig. 1 *A* and *C*) with significantly ($P < 0.05$) reduced pulmonary collagen deposition and, more specifically, less fibrosis within the egg granuloma of these mice (Fig. 1 *B* and *C*). In addition, in the absence of functional IL-25 there was reduced relative pulmonary expression of type 2 cytokines IL-4 and IL-13 (Fig. 1*D*), and reduced expression of TGFβ (Fig. 1*D*). Whereas pulmonary levels of IL-17A were up-regulated in response to *S. mansoni* eggs in WT mice, as previously demonstrated (2), there were comparable IL-17A levels in all groups (Fig. 1*D*). Regarding the reduction in IL-4 expression, a cytokine shown to be important in the generation of egg-associated granuloma formation (20), in

Significance

Abnormal damage and scarring of tissue (fibrosis) in the lungs can lead to pulmonary fibrosis. Patients that develop the various forms of pulmonary fibrosis are difficult to treat and have a high level of mortality. In this study we have used mouse models to address the role of the cytokine interleukin (IL)-25 and type 2 innate lymphoid cells (ILC2) in pulmonary fibrosis. In animal models we show a role for IL-25 and ILC2 in the generation of pulmonary fibrosis. Furthermore, we have identified elevated levels of IL-25 and ILC2s in the lungs of patients with idiopathic pulmonary fibrosis. This study provides insights on the factors and cells that may initiate pulmonary fibrosis in humans and have therapeutic potential.

Author contributions: E.H. and P.G.F. designed research; E.H., M.E.A., J.L.B., S.P.S., C.S., G.C., and R.J. Flynn performed research; G.C., R.J. Fahy, T.B.C., N.H., R.J. Flynn, D.V., A.N.J.M., and S.C.D. contributed new reagents/analytic tools; E.H., M.E.A., J.L.B., S.P.S., R.J. Flynn, and A.N.J.M. analyzed data; and E.H. and P.G.F. wrote the paper.

The authors declare no conflict of interest.

This article is a PNAS Direct Submission. S.K. is a guest editor invited by the Editorial Board.

[1]To whom correspondence should be addressed. E-mail: pfallon@tcd.ie.

This article contains supporting information online at www.pnas.org/lookup/suppl/doi:10.1073/pnas.1315854111/-/DCSupplemental.

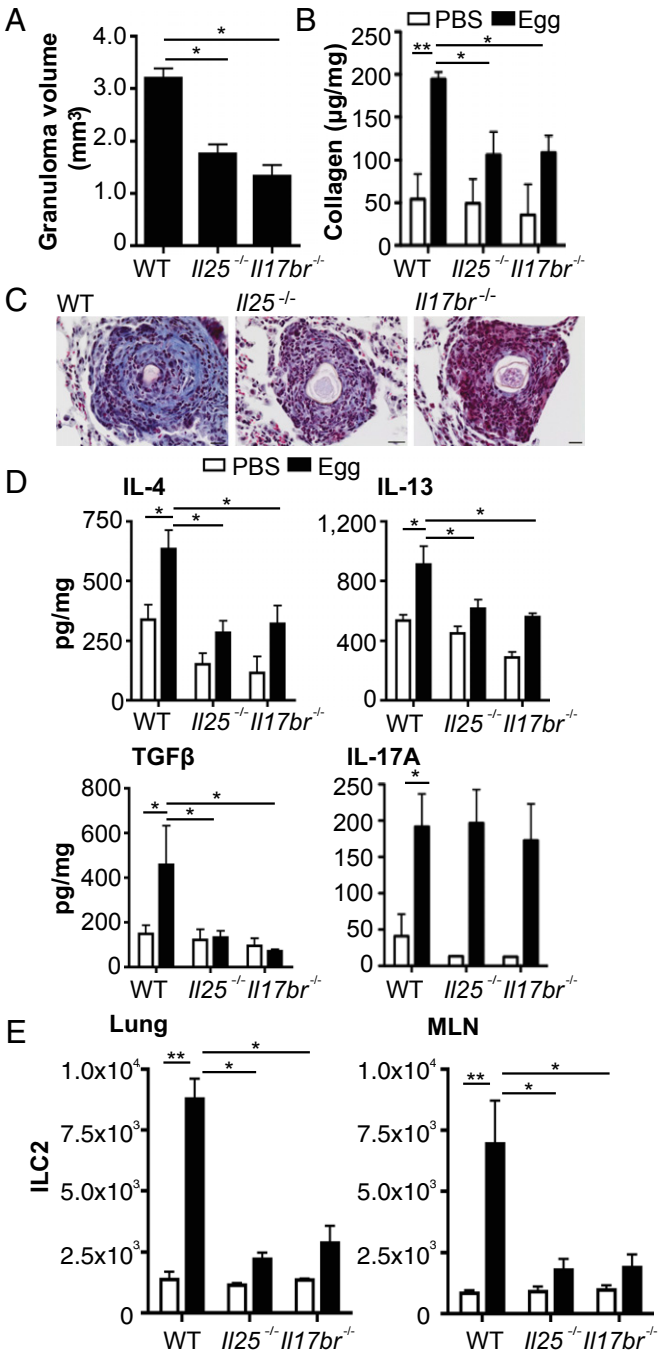

Fig. 1. Decreased pulmonary collagen deposition in IL-25–deficient mice following *S. mansoni* egg challenge. Pulmonary granulomas were induced in WT, *Il25*, and *Il17br* deficient mice. (*A*) Egg granuloma volume on hematoxylin and eosin-stained slides. (*B*) Total lung collagen expressed per mg of lung protein. (*C*) Representative histology images depicting collagen deposition within the granuloma using Masson's Trichrome stain (scale, 20 μM). (*D*) Levels of IL-4, IL-13, TGFβ, and IL-17A in lung digests expressed per mg of lung protein. (*E*) Expression of ILC2 [lineage (CD3, CD4, CD8, CD11b, CD11c, CD19, Gr-1, F4/80, FcεR1)$^-$IL-7Rα$^+$Sca-1$^+$T1/ST2$^+$ICOS$^+$] in lungs and MLN. Data are representative of mean ± SEM (n = 3–10) from three individual experimental replicates (*P < 0.05, **P < 0.01).

lungs of IL-25–deficient mice all groups had comparable infiltration of CD4$^+$ T cells (Fig. S1*A*), with no reduction in IL-4$^+$ Th2 cells in lungs of IL-25–deficient mice (Fig. S2*A*). In addition to CD4$^+$ T cells, basophils are an early source of IL-4 and IL-13 in innate type 2 responses (21, 22). However, we found no infiltration of basophils into the lungs in this model (Fig. S1*B*); indeed, following egg challenge of basophil-deficient mice (23) there was no defect in the development of pulmonary fibrosis (Fig. S1*C*).

Recent studies have highlighted the role for ILCs, in particular type 2 ILCs (ILC2) in helminth-associated type 2 immunity, with such cells potent producers of IL-13 during inflammation (11). Assessment of ILC2 in the *S. mansoni* egg-induced model of pulmonary inflammation demonstrates a significant (P < 0.01) increase in ILC2 in both the lung and mediastinal lymph node (MLN) of egg-challenged WT mice, with reduced number of ILC2s in the lungs of egg-challenged *Il25*$^{-/-}$ and *Il17br*$^{-/-}$ mice (Fig. 1*E*). In the lungs of WT mice, the frequency of IL-13$^+$ILC2 peaked at day 7, with expression of such cells approximately fivefold higher than IL-13$^+$CD4$^+$ T cells, with diminished IL-13$^+$ ILC2 in the absence of IL-25 (Fig. S2*B*), whereas in the MLN CD4$^+$ T cells are the primary source of IL-13 in both the presence and absence of IL-25 (Fig. S2*C*).

In addition to IL-25, ILC2 are induced by the type 2 cytokines IL-33 and thymic stromal lymphopoietin (TSLP) (24). Although other studies have shown that IL-33 is the more prominent cytokine involved in the induction of ILC2 (25), in this model we show that whereas IL-25 is significantly (P < 0.05) up-regulated in the lungs in response to *S. mansoni* eggs, the levels of IL-33 and TSLP in the lungs are markedly lower (Fig. S3*A*). In addition, in *Il17br*$^{-/-}$, but not animals with defective IL-33 (*Il1rl1*$^{-/-}$) or TSLP (*Tslpr*$^{-/-}$) signaling, there was a significant defect in egg-associated pulmonary collagen deposition (Fig. S3*B*). Furthermore, in the bleomycin model of pulmonary fibrosis, there is also reduced collagen deposition in the lungs of IL-25–deficient mice, with a corresponding reduction in IL-4 and IL-13 but not TGFβ or IL-17A (Fig. S4). In combination, these data show impaired collagen deposition in the absence of IL-25 in two different models of pulmonary fibrosis.

Absence of ILC2 Impairs the Development of Pulmonary Fibrosis and Associated Cytokine Production. Data presented thus far demonstrate a role for IL-25 in pulmonary fibrosis and potential involvement of ILC2. To address the role of ILC2 in pulmonary fibrosis, ILC2-deficient staggerer (*Rora*$^{sg/sg}$) mice, which have RORα deficiency, were used (26). ILC2-deficient *Rora*$^{sg/sg}$ mice (Fig. S5*A*) had no increase in pulmonary collagen deposition compared with WT mice following *S. mansoni* egg injection (Fig. S5*B*). Furthermore, *Rora*$^{sg/sg}$ bone marrow (BM) chimeras also had defects in pulmonary fibrosis (Fig. S5 *C* and *D*). To further investigate the role of ILC2 in the generation of pulmonary fibrosis, IL-25 was introduced intranasally to WT and *Rora*$^{sg/sg}$ mice to expand ILC2 in the lungs. IL-25 treatment elicited significant (P < 0.05) collagen deposition in the lungs of WT but not *Rora*$^{sg/sg}$ mice (Fig. 2 *A* and *B*). IL-25–elicited pulmonary fibrosis was associated with a significant increase in IL-13 (P < 0.01) and TGFβ (P < 0.05) in the lungs of WT mice, which was not apparent in *Rora*$^{sg/sg}$ mice (Fig. 2*C*).

Recent studies into the functions of ILCs have used an anti-CD90.2 mAb to block CD90.2 expressing ILC in *Rag1*$^{-/-}$ mice (27, 28). To determine the role of ILCs in innate fibrosis in the presence of CD4$^+$ T cells, lymphocyte-replete chimeras were generated by transfer of CD90.1 expressing T (CD3$^+$) and B (CD19$^+$) cells in to *Rag1*$^{-/-}$ mice expressing the CD90.2 allele (29). These mice were treated with anti-CD90.2 mAb or isotype-control mAb 1d before egg injection, and every 3 d thereafter to maintain ILC depletion. We initially confirmed that anti-CD90.2 mAb treatment effectively blocked ILC2 induction (P < 0.05) in the lungs in egg-injected mice, while maintaining CD4$^+$ T-cell induction (Fig. 3*A*). Interestingly, whereas Rag-1–deficient mice failed to generate granulomas, confirming the importance of CD4$^+$ T cells in this model, *Rag1*$^{-/-}$ mice are capable of generating pulmonary fibrosis independent of CD4$^+$ cells (Fig. 3*B*). However, following reconstitution with CD90.1$^+$ lymphocytes *Rag1*$^{-/-}$ mice develop larger pulmonary egg granulomas

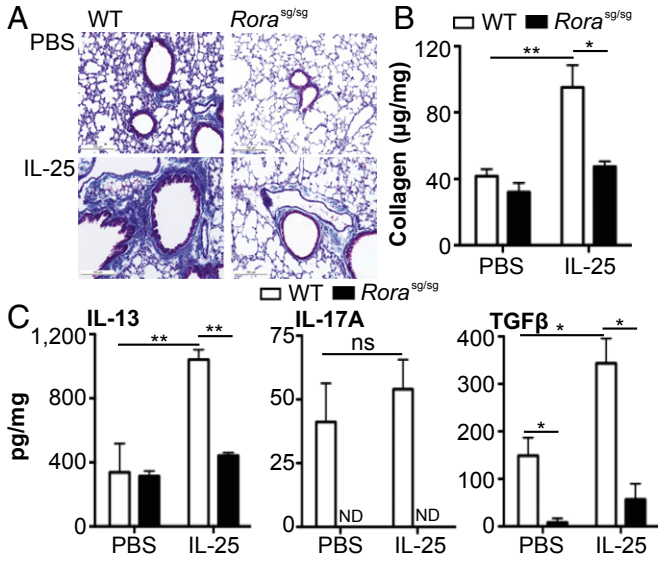

Fig. 2. IL-25 induces pulmonary collagen deposition in WT but not *Rora*$^{sg/sg}$ mice. WT and *Rora*$^{sg/sg}$ were treated with recombinant mouse IL-25 i.n. on days 0, 3, 7, 10, and 13. (*A*) Representative histology images depicting collagen deposition within the lung using Masson's Trichrome stain (scale, 100 μM). (*B*) Total collagen in lung digests expressed per mg of lung protein. (*C*) Levels of IL-13, IL-17A, and TGFβ in lung digests expressed per mg of lung protein. Data are representative of mean ± SEM (n = 3–5) from two individual experimental replicates (ns, not significant; *P < 0.05, **P < 0.01).

with significant fibrosis (Fig. 3*B*). In anti-CD90.2 mAb-treated CD90-disparate *Rag-1*$^{-/-}$ chimeric mice, the deficiency in ILC2 was accompanied by significantly reduced granuloma and impaired generation of pulmonary fibrosis relative to mAb-isotype control-treated mice (Fig. 3 *B* and *C*). The impaired collagen deposition in the absence of ILC2 was also associated with a significant decrease in pulmonary expression of IL-13 (P < 0.05) but not IL-4, TGFβ, or IL-17A (Fig. 3*D*). These data suggest that specific depletion of ILCs can abrogate *S. mansoni* egg-induced pulmonary fibrosis.

IL-13 Expression in ILC2 Induces Pulmonary Fibrosis in *S. mansoni* Egg-Challenged Mice. To directly confirm that ILC2 can elicit pulmonary fibrosis via their production of IL-13, we transferred ILC2 from *Il13*$^{-/-}$ or WT mice into *Il13*$^{-/-}$ during egg challenge; *Il13*$^{-/-}$ were used as these mice do not develop lung fibrosis in response to *S. mansoni* eggs (30, 31). Transfer of WT ILC2 induced collagen deposition in unchallenged mice, with marked fibrosis in egg-challenged mice receiving ILC2 (Fig. 4). In contrast, transfer of IL-13–deficent ILC2 did not induce collagen deposition in either challenged or unchallenged mice (Fig. 4). Therefore, using cell transfer studies we demonstrate that ILC2 can induce pulmonary fibrosis in an IL-13-dependent manner.

IL-25 and ILC2 Are Present in the Bronchalveolar Lavage and Lung Tissue of Patients with IPF. Data presented herein indicate a role for IL-25 in the generation of pulmonary fibrosis in murine models. To investigate the potential for IL-25 to play a role in the generation of clinical pulmonary fibrosis, we assessed IL-25 expression in the bronchalveolar lavage (BAL) fluid of a cohort of patients with IPF and control BAL samples from early-stage erythema nodosum patients, with the lungs clear of fibrotic lesions. The levels of IL-25 were significantly (P < 0.01) increased in the BAL fluid of IPF patients relative to control patients at first diagnosis (Fig. 5*A*). Furthermore, IL-25 levels were further enhanced in the same patients 1 y after diagnosis (Fig. 5*A*). Whereas other cytokines analyzed (IL-1β, IL-2, IL-4, IL-5, IL-8, IL-12p70, IL-13, IL-17A, IFNγ, and TNFα) were not

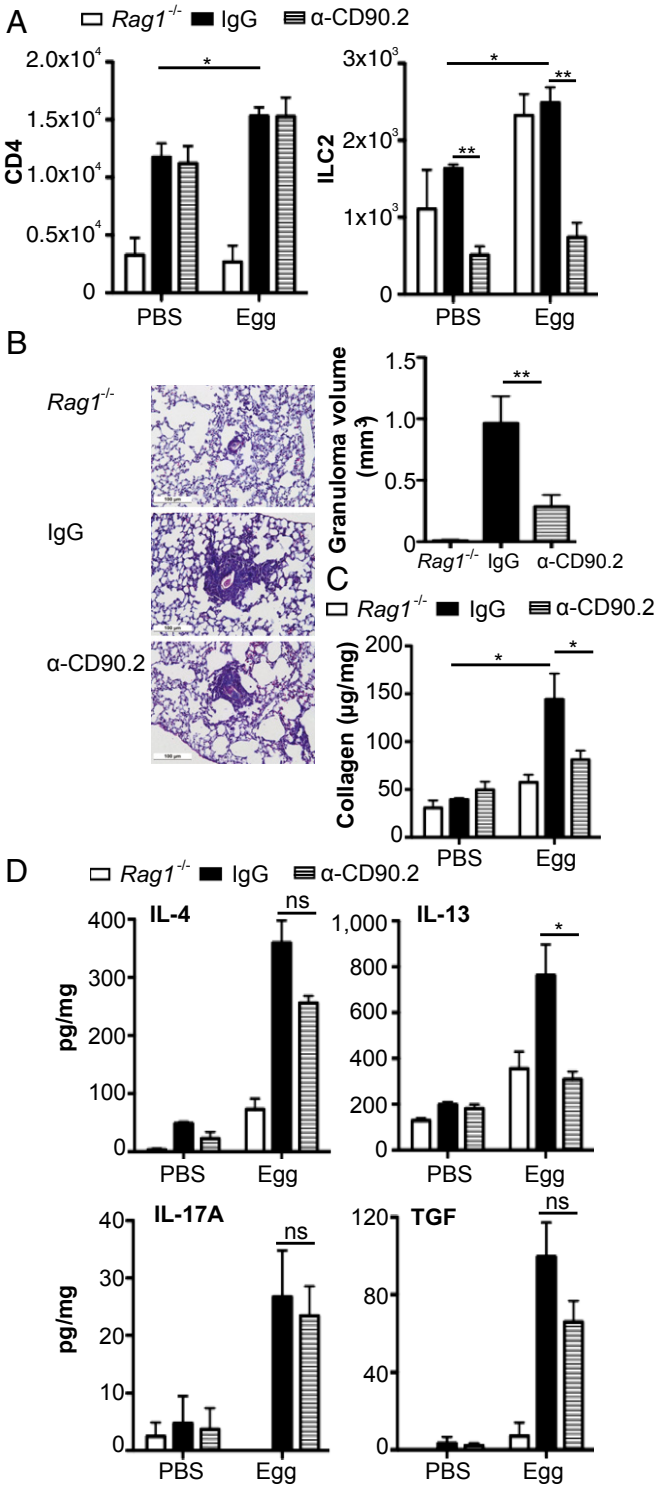

Fig. 3. ILC2 regulate pulmonary collagen deposition. Disparate CD90 chimeras were generated by transferring CD90.1 T (CD3$^+$) and B (CD19$^+$) cells to *Rag-1*$^{-/-}$ mice expressing the CD90.2 allele, which were subsequently treated with anti-CD90.2 or an isotype control mAb. (*A*) Lung frequency of CD4 and ILC2 in *Rag-1*$^{-/-}$, disparate CD90 chimeras treated with anti-IgG and disparate CD90 chimeras treated with anti-CD90.2. (*B*) Granuloma volume and representative histology images stained with Masson's Trichrome (scale, 100 μM). Lung collagen (*C*) and cytokines (*D*) expressed per mg of lung protein. Data are representative of mean ± SEM (n = 3–5) from two individual experimental replicates (ns, not significant; *P < 0.05, **P < 0.01).

IMMUNOLOGY

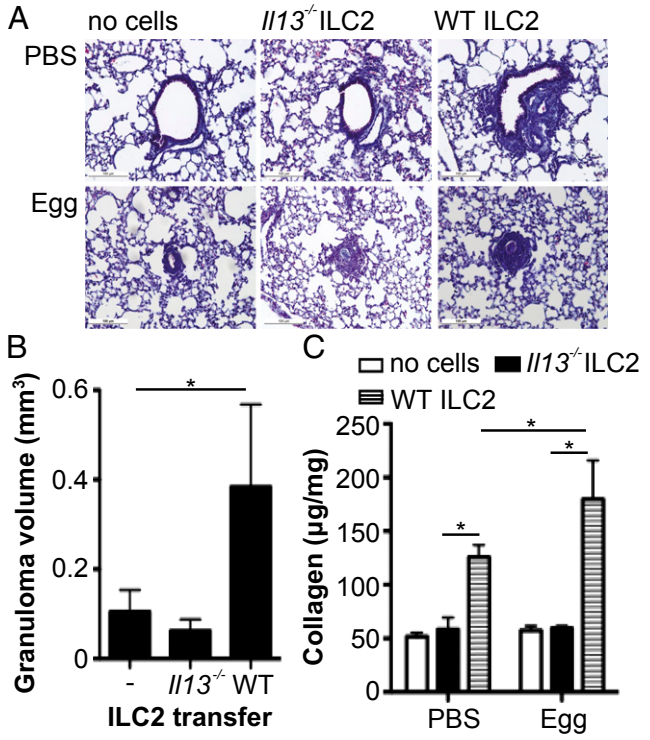

Fig. 4. Transferring IL-13–expressing ILC2 induces pulmonary collagen deposition in IL-13–deficient mice. ILC2 isolated from WT and *Il13*$^{-/-}$ were transferred into unchallenged and egg-challenged IL-13–deficient mice. (*A*) Representative histology images depicting Masson's Trichrome staining from PBS and egg-challenged animals (scale, 100 μM) and (*B*) egg-associated granuloma volume. (*C*) Lung collagen expressed per mg of lung protein. Data are representative of mean ± SEM (n = 2–4) from two individual experimental replicates (*$P < 0.05$).

significantly enhanced at initial diagnosis, these cytokines were significantly ($P < 0.01$–0.05) elevated in the BAL 1-y post-diagnosis (Fig. 5*A* and Fig. S6 *A* and *B*). Interestingly, levels of IL-25 showed a moderate positive correlation ($P < 0.05$; $R = 0.3748$) with periostin levels, an extracellular matrix protein associated with IPF and lung remodeling (32), in BAL from IPF patients (Fig. 5*B*). As the mouse data showed infiltration of ILC2 in lungs of mice with pulmonary fibrosis (Fig. 1*E*), we investigated if ILC2 cells were in patients with IPF. A population of lineage marker (CD3, CD4, CD8, CD11b, CD11c, CD14, CD19, CD56, CD123, FcεR1) negative cells that expressed CRTH2, T1/ST2, CD45, ICOS, IL-7Rα, and IL-17BR was significantly ($P < 0.05$) enhanced in the BAL of IPF patients compared with control patients (Fig. 5*C*). The ILC2 population in IPF patients is similar to those previously seen in human lung tissue and BAL (16, 27), but this is an observation of these cells in association with pulmonary fibrosis.

Discussion

Pulmonary fibrotic conditions are common and often are associated with poor prognosis. The pathogenesis of pulmonary fibrosis is not fully understood, with theories based on either a recurrent inflammatory response and subsequent tissue destruction and wound healing (33), or a single inflammatory phase rapidly followed by aberrant wound healing (34). Studies into the pathogenesis of pulmonary fibrosis have primarily focused on the classical profibrotic cytokines TGFβ, and more recently, IL-13. Herein we demonstrate a role for the type 2 cytokine IL-25 and IL-25–elicited ILC2 in pulmonary fibrosis in murine models. Furthermore, in a small cohort of IPF patients there was increased IL-25 in the presence of lung fibrosis and an up-regulation of ILC2 in the BAL fluid, inferring a potential role for IL-25 and ILC2 in human disease.

Murine data have already provided evidence on both the role of type 2 cytokines and innate lymphoid cells on the progression of inflammation and fibrosis at several mucosal sites (11, 12, 27, 28). Data presented herein demonstrate the ability of IL-25 to drive fibrosis, confirmed by a decrease in collagen deposition in the absence of functional IL-25 signaling in two independent models of pulmonary fibrosis. One mechanism potentially underlying these observations involves ILC2-derived IL-13 expression, confirmed by the ability of transferred ILC2 to induce pulmonary fibrosis in an IL-13–dependent manner. Indeed, to demonstrate the role of ILC2 in the progression of pulmonary fibrosis we adopted several independent methods, using mice deficient in RORα, RORα chimeras as well as blocking CD90.2-expressing ILCs. In these mouse models a role for ILC2 in pulmonary fibrosis was shown. As there are currently no effective models for specifically blocking ILC2 in vivo, without also inhibiting other CD90-expressing cell types such as other ILC populations or innate cells such as basophils, these results could be further interrogated once an effective specific blocking protocol is developed.

We show that in the absence of IL-25 there is a decreased expression of the Th2 cytokine IL-4 and the profibrotic cytokine TGFβ, in addition to IL-13, despite comparable IL-4^{+}Th2 cell expression between groups. Analysis of the cell populations associated with the egg-induced pulmonary granuloma suggests ILC2 are a major source of IL-13, which is absent in IL-25–deficient mice, whereas the frequency of IL-4^{+}CD4^{+} was comparable in WT- and IL-25–deficient mice. Further work is required to address the reduced TGFβ in lungs of IL-25–deficient mice in the *S. mansoni* egg-induced model of pulmonary fibrosis, which is not apparent in the bleomycin model. Interestingly, IL-25 treatment was shown to directly elicit TGFβ in the lungs of WT mice. Studies on human fibroblasts, known as a prominent source of TGFβ in wound healing and fibrosis (35), have shown that fibroblasts respond to IL-25, they express IL-17BR, and produce TGFβ (36). These observations taken in combination with the apparent role for IL-25 in promoting fibrosis suggest this could be an interesting avenue for further mechanistic research in mice. Interestingly, in the models we have used, whereas we observe increased IL-17A in response to egg challenge in WT mice, as reported previously (2), pulmonary levels of IL-17A are not altered in the absence of IL-25 or ILC2. In addition, despite noting a general increase in the frequency of ILCs in the lungs of challenged mice; we do not observe an increase in IL-17–producing ILC3, with the source of IL-17 detected in the lungs being Th17 cells.

Using a small cohort of IPF patients we observed that the increased expression of IL-25 in BAL has a moderate correlation with the levels of periostin, a marker recently shown to promote fibrosis in IPF patients (32). In accordance with previous studies, we also show increased expression of other cytokines, such as IL-8, IL-4, IL-1β, and IL-17A in the BAL of IPF patients (2). In addition, we show increased expression of ILC2 in the BAL of IPF patients compared with BAL from patients without pulmonary fibrosis. ILC2 have previously been identified both in healthy lung tissue and tissue from asthma, rhinosinitis, and influenza patients (16), implying a role for these cells in pulmonary inflammation. Whereas the human data presented herein provide a tantalizing insight into the potential role of IL-25 and ILC2 in fibrosis, confirmation of the observations we have seen would be required in a larger cohort of patients before any firmer conclusions are made. This study highlights a unique role for IL-25 and ILC2 in pulmonary conditions and identifies therapeutic targets for fibrosis in the human lung as well as other chronic fibrotic disorders.

Materials and Methods

Animals. Bagg albino (BALB/c) and C57BL/6 mice were purchased from Harlan. IL-25– (10), IL-17BR– (11), T1/ST2- (37), TSLPR- (38), IL-13– (39), and

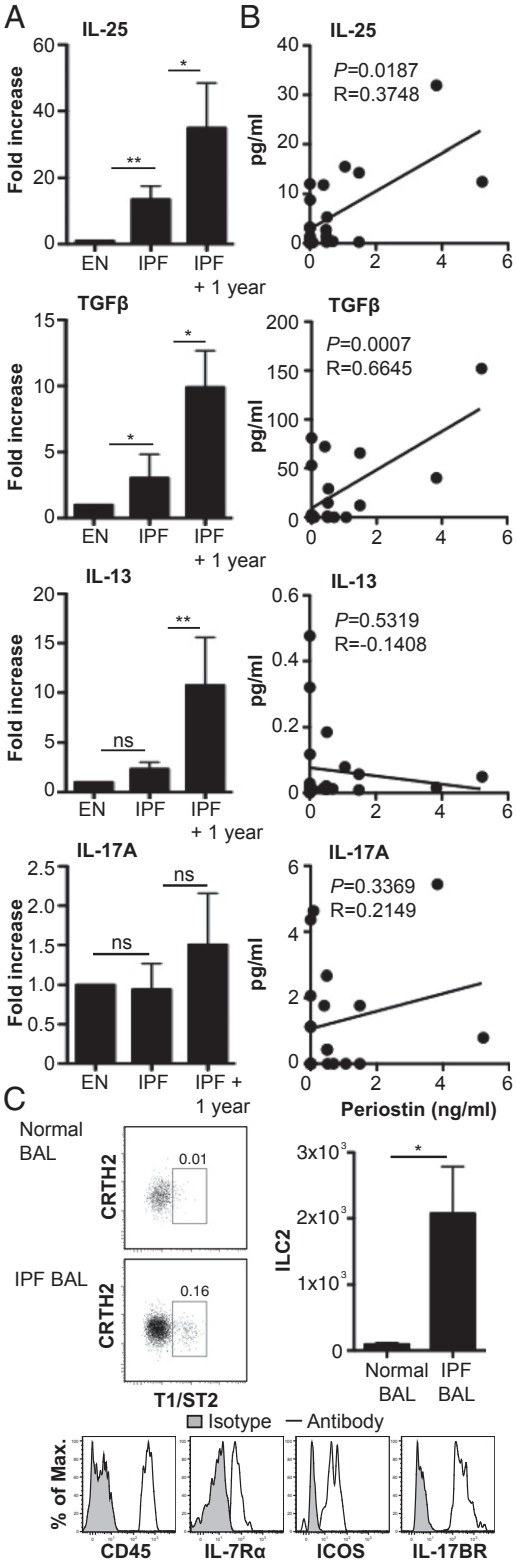

Fig. 5. IPF patients have increased expression of IL-25 and ILC2 in the BAL. BAL fluid was collected from patients with IPF at diagnosis and at a 1-y follow-up (IPF + 1 y) and patients diagnosed with erythema nodosum (EN; nonprogressive patients). (*A*) IL-25, IL-13, TGFβ, and IL-17A in BAL fluid expressed as fold-increase relative to EN patients. (*B*) Correlation between BAL fluid levels of IL-25, IL-13, TGFβ, or IL-17A and periostin was plotted and Pearson's correlation calculated and displayed on the graph. (*C*) Representative plots of ILC2 [lineage (CD3, CD4, CD8, CD11b, CD11c, CD19, CD14, CD56, CD123, FcεR1) negative, expressing CRTH2, T1/ST2, CD45, ICOS, IL-7Rα, and IL-17BR] in the BAL of nonfibrotic patients and IPF patients, with expression of these cells displayed as a percentage of live cells per sample. Data are representative of mean ± SEM ($n = 3$, EN; $n = 14$, IPF and IPF + 1 y) (ns, not significant; $^*P < 0.05$, $^{**}P < 0.01$).

staggerer-*Rora*$^{sg/sg}$–deficient mice (Jackson Laboratories) were bred in-house on a BALB/c background. *Rag-1*–deficient mice and CD90.1$^+$ mice and CD45.1$^+$ on a C57BL/6 background were obtained from Jackson Laboratories and bred in-house. *Mcpt8Cre* mice (23) experiments were performed in the Department of Infection Biology, Universitätsklinikum Erlangen, Germany. In all studies, female mice of 8–12 wk of age were used, with the exception of *Rora*$^{sg/sg}$, which were used at 4–5 wk of age. All animal experiments were performed in compliance with Irish Department of Health and Children regulations and approved by the Trinity College Dublin's BioResources ethical review board, or the UK Home Office.

***S. mansoni* Egg-Induced Pulmonary Granuloma Formation and Antibody Treatment.** *S. mansoni* eggs were isolated from the livers of mice infected with *S. mansoni,* and pulmonary granulomas were induced by i.v. injection of 5,000 *S. mansoni* eggs (40). For neutralizing experiments anti-CD90.2 mAb (30H12; BioXCell), or rat IgG2b isotype control, was administered i.p. every 3 d at a dose of 250 μg per mouse starting 1 d before i.v. egg administration.

Bleomycin- and IL-25–Induced Pulmonary Fibrosis. Pulmonary fibrosis was induced by intratracheal injection of 0.15 U bleomycin (Sigma), as previously described (2). Mice were given 0.5 μg recombinant mouse IL-25 intranasal (i.n.) on days 0, 3, 7, 10, and 13 and lung tissue and MLN harvested on day 14.

IPF Study Subjects. All IPF subjects ($n = 14$) were Caucasian and provided written informed consent. Ethical approval was obtained from the Lothian Research Ethics Committee. IPF was diagnosed according to the American Thoracic Society/European Respiratory Society bases on multidisciplinary consensus classification. Surgical lung biopsy and/or BAL was performed as described previously (41). Baseline characteristics of IPF patients, in addition to characteristics at 1-y follow-up, are presented in Table S1.

Erythema Nodosum Patients. Irish patients were diagnosed at initial hospital presentation by the same physician (S.C.D.). All patients were classified at presentation using chest radiograph (staged 0–IV, i.e., normal to fibrosis), in accordance with the Siltzbach staging system as per international guidelines. BAL samples from patients that were subsequently diagnosed with erythema nodosum ($n = 3$) served as a control group in this study. Ethical approval for the study was obtained from the St. Vincent's University Hospital Medical Ethics Committee. Informed written consent was obtained from all participants.

Lung Tissue Processing and Histology. Lung tissue from mice or biopsy samples taken from IPF patients was perfused and fixed in 10% formalin saline, then paraffin-embedded. Healthy control slides of human lung were from Imgenex. Paraffin-embedded sections were cut to 4 μM and the slides stained with hematoxylin and eosin or Masson's trichrome to assess pulmonary fibrosis. Histology was imaged using an Olympus BX43 with an Olympus DP25 Camera.

Lung tissue from mice was collected for cytokine and collagen analysis. Tissue was homogenized and prepared as previously described (42). Lung collagen was analyzed using the Sircol collagen assay (Biocolor Life Science Assays) as described (43).

Flow Cytometry. Surface marker expression was assessed by flow cytometry with data collection on a CyAn (Beckman Coulter). Data were analyzed using FlowJo software (Tree Star). Murine cells were stained with BD Biosciences mAbs; CD8-APC (Ly-2), B220-APC (RA3-6B2), F4/80-APC (BM8), ICOS-PE (7E.17G9), Siglec-F-APC (E50-2440), Sca-1-PE-Cy7 (D7), c-kit-PE (2B8), eBiosciences mAbs; CD4-APC (RM4-5), CD11b-APC (M1/70), Gr-1-APC (RB6-8CS), FcεR1-APC (MAR-1), IL-7Rα-APC-Cy7 (A7R34), BioLegend mAb; LAP (TGF-β1)-PE (TW7-16B4), and MD biosciences mAb; T1/ST2-FITC (DJ8). For intracellular cytokine, staining cells were cultured with 50 ng/mL phorbol 12-myristate 13-acetate and 500 ng/mL ionomycin in the presence of 10 μg/mL Brefeldin A for 4 h. Permeabolized cells were stained with eBiosciences mAb; IL-4-PerCP-efluor 710 (11B11), IL-5-PE (TRFK5), IL-13-efluor 450 (eBio13A), and BD Biosciences mAb; IL-17A-PE (TC11-18H10). Human cells were stained with BD Biosciences mAbs; CD3-PerCP (SK7), CD19-PerCP (SJ25C1), CD14-PerCP (MΦP9), CD45-AlexaFluor 700 (HI30) CD56-PECy7 (B159), eBiosciences mAbs; CD11c-PerCP (3.9), CD123-PerCP (6H6), CD127-APC (eBioRDR5), Biolegend mAbs; CD8a-PerCP (RPA-T8), FcεR1a-PerCP (AER-37(CRA-a)), CRTH2-PE (BM16),

ICOS-Pacific blue (C398.4A), Abcam mAb; CD11b-PerCP (DCIS1/18), MD Biosciences mAb; ST2-FITC (B4B6), and R&D Systems mAb; IL-17BR-APC (170220). Using appropriate isotype controls, quadrants were drawn and data were plotted on logarithmic-scale density- or dot plots.

ILC2 Cell Sorting. BALB/c *Il13*$^{+/+}$ or *Il13*$^{-/-}$ mice were treated with 2 μg recombinant mouse IL-25 i.p. for 3 d and the peritoneal exudate cells were collected and stained for ILC2 isolation. Cells were sorted on a Mo-Flo cell-sorter-based ILC2 population (lineage^{-}(CD3, CD4, CD8, CD19, CD11b, CD11c, Gr-1, FcεR1, F4/80)ICOS^{+}T1/ST2^{+}), which revealed a purity of >90% live cells. Isolated cells were injected i.p. into *Il13*$^{-/-}$ mice at a concentration of 200,000 cells per mouse.

CD90 Disparate *Rag-1*$^{-/-}$ Chimera Generation. CD90 disparate chimeras were generated using methods previously described (29). Briefly, 6×10^7 purified B- (CD19^{+}) and T (CD3^{+}) cells were isolated from the spleen, and lymph nodes from CD90.1^{+} mice were transferred i.v. into CD90.2 *Rag-1*$^{-/-}$ mice. After 8 wk reconstitution was confirmed by examination of peripheral blood lymphocytes.

BM Chimera Generation. Lethally irradiated CD45.1^{+} C57BL/6 recipient mice (9 Gy in two doses, 3 h apart) were reconstituted with 1×10^7 BM cells from CD45.2^{+} C57BL/6 mice or *Rora*$^{sg/sg}$ mice. To ensure efficient irradiation and reconstitution, expression of CD45.1 vs. CD45.2 was assessed in the blood after 4 wk. After 6 wk C57B6/J mice reconstituted with WT or *Rora*$^{sg/sg}$ BM were injected with 5,000 *S. mansoni* eggs i.v. and lung tissue harvested after 7 d.

Mouse Cytokine ELISAs. For enumeration of cytokines, murine lung sections were prepared by homogenization as previously described (42). Samples were analyzed by sandwich ELISAs to quantify levels of specific cytokines. All murine cytokines (IL-1β, IL-4, IL-13, IL-17, IL-33, IFNγ, TNFα, and TGFβ) were measured with the DuoSet ELISA development system from R&D Systems following the manufacturer's protocol. Expression of all lung proteins is expressed per mg lung protein present.

Human Cytokine and Periostin ELISAs. Concentrations of IL-25 were determined in human BAL fluid by ELISA (Cusabio Biotech) according to manufacturer's instructions. Levels of human periostin in BAL fluid were measured using a sandwich ELISA kit from Holzel Diagnostika following the manufacturer's instructions. IL-17A in patients BAL fluid was quantified using a human cytokine assay from MesoScale Discovery (MSD, ultrasensitive kit). Levels of all other cytokines were assessed in BAL fluid in this study using a Th1/Th2 10-Plex multiplex cytokine assay (MSD) according to manufacturer's instructions. Results for cytokine levels in BAL fluid were standardized per ml of fluid recovered during the lavage process. Results are expressed as fold-increase relative to basal cytokines detected in BAL of erythema nodosum patients.

Statistics. Statistical analysis was performed using GraphPad and InStat. Results are presented as mean ±SEM. Differences, indicated as two-tailed *P* values, were considered significant when $P < 0.05$ was assessed by unpaired Student *t* test with Welch correction applied as necessary. Pearson's correlation was performed on BAL fluid data comparing periostin and cytokine levels; a *P* value of less than 0.05 was considered significant.

ACKNOWLEDGMENTS. The authors thank Dr. Malgorzata Kubica for her assistance with this article. This work was supported by Science Foundation Ireland (P.G.F. and S.C.D.), National Children's Research Centre (P.G.F.), Health Research Board of Ireland (P.G.F. and S.C.D.), and Asthma UK (A.N.J.M.).

1. Ley B, et al. (2012) A multidimensional index and staging system for idiopathic pulmonary fibrosis. *Ann Intern Med* 156(10):684–691.
2. Wilson MS, et al. (2010) Bleomycin and IL-1beta-mediated pulmonary fibrosis is IL-17A dependent. *J Exp Med* 207(3):535–552.
3. Wynn TA (2011) Integrating mechanisms of pulmonary fibrosis. *J Exp Med* 208(7): 1339–1350.
4. Noble PW, Barkauskas CE, Jiang D (2012) Pulmonary fibrosis: Patterns and perpetrators. *J Clin Invest* 122(8):2756–2762.
5. Chiaramonte MG, et al. (1999) IL-13 is a key regulatory cytokine for Th2 cell-mediated pulmonary granuloma formation and IgE responses induced by Schistosoma mansoni eggs. *J Immunol* 162(2):920–930.
6. Fallon PG, Richardson EJ, McKenzie GJ, McKenzie AN (2000) Schistosome infection of transgenic mice defines distinct and contrasting pathogenic roles for IL-4 and IL-13: IL-13 is a profibrotic agent. *J Immunol* 164(5):2585–2591.
7. Wynn TA (2003) IL-13 effector functions. *Annu Rev Immunol* 21:425–456.
8. Kraft M (2011) Asthma phenotypes and interleukin-13—moving closer to personalized medicine. *N Engl J Med* 365(12):1141–1144.
9. Barron L, Wynn TA (2011) Fibrosis is regulated by Th2 and Th17 responses and by dynamic interactions between fibroblasts and macrophages. *Am J Physiol Gastrointest Liver Physiol* 300(5):G723–G728.
10. Fallon PG, et al. (2006) Identification of an interleukin (IL)-25-dependent cell population that provides IL-4, IL-5, and IL-13 at the onset of helminth expulsion. *J Exp Med* 203(4):1105–1116.
11. Neill DR, et al. (2010) Nuocytes represent a new innate effector leukocyte that mediates type-2 immunity. *Nature* 464(7293):1367–1370.
12. Saenz SA, et al. (2010) IL25 elicits a multipotent progenitor cell population that promotes T(H)2 cytokine responses. *Nature* 464(7293):1362–1366.
13. Moro K, et al. (2010) Innate production of T(H)2 cytokines by adipose tissue-associated c-Kit(+)Sca-1(+) lymphoid cells. *Nature* 463(7280):540–544.
14. Price AE, et al. (2010) Systemically dispersed innate IL-13-expressing cells in type 2 immunity. *Proc Natl Acad Sci USA* 107(25):11489–11494.
15. Corrigan CJ, et al. (2011) Allergen-induced expression of IL-25 and IL-25 receptor in atopic asthmatic airways and late-phase cutaneous responses. *J Allergy Clin Immunol* 128(1):116–124.
16. Mjösberg JM, et al. (2011) Human IL-25- and IL-33-responsive type 2 innate lymphoid cells are defined by expression of CRTH2 and CD161. *Nat Immunol* 12(11):1055–1062.
17. Angkasekwinai P, et al. (2007) Interleukin 25 promotes the initiation of proallergic type 2 responses. *J Exp Med* 204(7):1509–1517.
18. Fort MM, et al. (2001) IL-25 induces IL-4, IL-5, and IL-13 and Th2-associated pathologies in vivo. *Immunity* 15(6):985–995.
19. Ballantyne SJ, et al. (2007) Blocking IL-25 prevents airway hyperresponsiveness in allergic asthma. *J Allergy Clin Immunol* 120(6):1324–1331.
20. Pearce EJ, et al. (1996) Schistosoma mansoni in IL-4-deficient mice. *Int Immunol* 8(4): 435–444.
21. Min B, et al. (2004) Basophils produce IL-4 and accumulate in tissues after infection with a Th2-inducing parasite. *J Exp Med* 200(4):507–517.
22. Wakahara K, et al. (2013) Basophils are recruited to inflamed lungs and exacerbate memory Th2 responses in mice and humans. *Allergy* 68(2):180–189.
23. Ohnmacht C, et al. (2010) Basophils orchestrate chronic allergic dermatitis and protective immunity against helminths. *Immunity* 33(3):364–374.
24. Hams E, Fallon PG (2012) Innate type 2 cells and asthma. *Curr Opin Pharmacol* 12(4): 503–509.
25. Barlow JL, et al. (2013) IL-33 is more potent than IL-25 in provoking IL-13-producing nuocytes (type 2 innate lymphoid cells) and airway contraction. *J Allergy Clin Immunol* 132(4):933–941.
26. Wong SH, et al. (2012) Transcription factor RORα is critical for nuocyte development. *Nat Immunol* 13(3):229–236.
27. Monticelli LA, et al. (2011) Innate lymphoid cells promote lung-tissue homeostasis after infection with influenza virus. *Nat Immunol* 12(11):1045–1054.
28. Sonnenberg GF, et al. (2012) Innate lymphoid cells promote anatomical containment of lymphoid-resident commensal bacteria. *Science* 336(6086):1321–1325.
29. Sonnenberg GF, Monticelli LA, Elloso MM, Fouser LA, Artis D (2011) CD4(+) lymphoid tissue-inducer cells promote innate immunity in the gut. *Immunity* 34(1):122–134.
30. Fallon PG, et al. (2002) IL-4 induces characteristic Th2 responses even in the combined absence of IL-5, IL-9, and IL-13. *Immunity* 17(1):7–17.
31. Kaviratne M, et al. (2004) IL-13 activates a mechanism of tissue fibrosis that is completely TGF-beta independent. *J Immunol* 173(6):4020–4029.
32. Naik PK, et al.; COMET Investigators (2012) Periostin promotes fibrosis and predicts progression in patients with idiopathic pulmonary fibrosis. *Am J Physiol Lung Cell Mol Physiol* 303(12):L1046–L1056.
33. Selman M, King TE, Pardo A; American Thoracic Society; European Respiratory Society; American College of Chest Physicians (2001) Idiopathic pulmonary fibrosis: Prevailing and evolving hypotheses about its pathogenesis and implications for therapy. *Ann Intern Med* 134(2):136–151.
34. Gauldie J, Bonniaud P, Sime P, Ask K, Kolb M (2007) TGF-beta, Smad3 and the process of progressive fibrosis. *Biochem Soc Trans* 35(Pt 4):661–664.
35. Wynn TA (2008) Cellular and molecular mechanisms of fibrosis. *J Pathol* 214(2):199–210.
36. Létuvé S, et al. (2006) IL-17E upregulates the expression of proinflammatory cytokines in lung fibroblasts. *J Allergy Clin Immunol* 117(3):590–596.
37. Townsend MJ, Fallon PG, Matthews DJ, Jolin HE, McKenzie AN (2000) T1/ST2-deficient mice demonstrate the importance of T1/ST2 in developing primary T helper cell type 2 responses. *J Exp Med* 191(6):1069–1076.
38. Al-Shami A, et al. (2004) A role for thymic stromal lymphopoietin in CD4(+) T cell development. *J Exp Med* 200(2):159–168.
39. McKenzie GJ, et al. (1998) Impaired development of Th2 cells in IL-13-deficient mice. *Immunity* 9(3):423–432.
40. Fallon PG, Emson CL, Smith P, McKenzie AN (2001) IL-13 overexpression predisposes to anaphylaxis following antigen sensitization. *J Immunol* 166(4):2712–2716.
41. Bournazos S, et al. (2011) Copy number variation of FCGR3B is associated with susceptibility to idiopathic pulmonary fibrosis. *Respiration* 81(2):142–149.
42. Mangan NE, Dasvarma A, McKenzie AN, Fallon PG (2007) T1/ST2 expression on Th2 cells negatively regulates allergic pulmonary inflammation. *Eur J Immunol* 37(5):1302–1312.
43. Amu S, et al. (2010) Regulatory B cells prevent and reverse allergic airway inflammation via FoxP3-positive T regulatory cells in a murine model. *J Allergy Clin Immunol* 125(5):1114–1124 e1118.